Nuclear Engineering and Design 56 (1980) 359–368

NUMERICAL SIMULATION OF THE TRANSIENT TEMPERATURE DISTRIBUTION INSIDE A CLOSE-PACKED ARRAY OF CYLINDRICAL TUBES DURING HEATING AND COOLING UNDER HIGH VACUUM

Sergio PISSANETZKY
*Centro Atómico Bariloche *, 8400 S.C. de Bariloche, R.N., Argentina*

Received 19 June 1979

The metallurgical processing of zircaloy for reactor fuel pin cladding requires the annealing of loads, each consisting of an array of tubes in a high-vacuum furnace. A knowledge of the transient temperature distribution in the load during the heating and cooling periods is of interest for the design of the furnace, the design of each load on account of the final yield of the furnace, and the metallurgical control of the process. A general mathematical model was devised, and is presented here, for the numerical simulation of heat transfer by radiation and conduction. The model was used to simulate the behaviour of loads consisting of a close-packed array of cylindrical tubes of two different diameters and wall thicknesses, and in one case with two different surface emissivities. The following processes were simulated: heating from an initial to a final temperature; pre-heating from an initial to an intermediate temperature; final heating from the intermediate to the final temperature, and cooling of the load. Numerous numerical results are presented and discussed in depth in order to get physical insight into the problem, and rules are formulated which are of great value to the engineer and the metallurgist.

1. Introduction

The metalurgical processing of zircaloy for reactor fuel pin cladding requires the repeated annealing of loads consisting of an array of cylindrical tubes. The annealing is usually performed in a large industrial furnace under a high vacuum in order to avoid damaging the surface of the metal. A detailed knowledge of the transient temperature distribution within the load during the heating and the cooling periods is of interest for:

(a) The design of the furnace.

(b) The analysis of the yield as a function of the load size. The innermost tubes of a large load may take a long time to reach the desired temperature.

(c) The metalurgical control of the annealing process.

In this publication a mathematical model is presented which was devised in order to calculate the temperature as a function of position and time within the load. The model is based on a general computer program which solves heat conduction problems by the method of finite elements and two-dimensional heat radiation problems for any given set of hot surfaces which are diffuse-gray radiators and reflectors. Because of the high vacuum, the model only considers heat transfer by conduction and radiation. The temperature distribution is assumed to be independent of the coordinate along the furnace and the problem is thus two-dimensional. The tubes are long and, due to slight imperfections, adjacent tubes touch each other only at few points along their length and the thermal contact between them is very poor; therefore the model neglects the heat conduction between adjacent tubes.

Several situations were modeled in order to get a better insight into the behaviour of the system, and numerous numerical results are presented and discussed here. The model consisted of a close-packed array of cylindrical tubes. The external part of the surface of all of the outermost tubes was kept at a constant temperature and the evolution of the temperature at every internal point of the array was calculated as a function of time until the external tem-

* Comisión Nacional de Energía Atómica.

perature was reached. These calculations were performed for both heating and cooling processes between different combinations of initial and final temperatures, for different emissivities of the surfaces and for tubes of different diameters and wall thicknesses.

The numerical techniques used here will be described in some detail because they are general and can be used to model a variety of situations involving heat conduction and radiation in two dimensions.

2. Finite element formulation of heat conduction

The finite element method [1] was used to solve the two-dimensional transient heat conduction problem in the tubes. One-dimensional finite elements were chosen because the temperature differences between the internal and the external surfaces of a tube were negligibly small. The finite element model for each tube has 12 elements and 12 nodes, and is shown in fig. 1, where the numbering of the elements and the nodes is shown, the numbers of the elements being encircled. The quasi-harmonic time-dependent differential equation for heat conduction in one dimension is [2]

$$\frac{\partial}{\partial x}\left(K\frac{\partial T}{\partial x}\right)+Q=\rho c\frac{\partial T}{\partial t}, \tag{1}$$

where

T is the temperature,

Q is the net heat which enters the element (divided by the volume of the element) as a result of the balance between the emission and the absorption of radiation at both surfaces of the element,

K is the (temperature dependent) heat conductivity;

c is the (temperature dependent) heat capacity, and

ρ is the density.

It is well known that eq. (1) can be solved by minimizing the functional

$$\chi=\int_V\frac{1}{2}\left[K\left(\frac{\partial T}{\partial x}\right)^2-2\left(Q-\rho c\frac{\partial T}{\partial t}\right)T\right]\mathrm{d}V. \tag{2}$$

The integral is calculated by dividing the body under consideration into one-dimensional elements, each with two nodes, and using a linear interpolation for the temperature within the element. The resulting expression is quadratic in the N nodal temperatures. The following set of N linear differential equations is obtained by equating to zero the derivatives of χ with respect to each of the nodal temperatures:

$$[C]\frac{\partial\{T\}}{\partial t}+[K]\{t\}+\{F\}=0, \tag{3}$$

where $\{T\}$ is now a column vector composed of the nodal temperatures, and $[C]$ and $[K]$ are $N\times N$ matrices and $\{F\}$ an $N\times 1$ vector obtained by assembling the following element matrices and vector [2]:

$$[c^{(e)}]=\frac{\rho cAL}{6}\begin{vmatrix}2 & 1\\ 1 & 2\end{vmatrix},$$

$$[k^{(e)}]=\frac{AK}{L}\begin{vmatrix}1 & -1\\ -1 & 1\end{vmatrix},$$

$$\{f^{(e)}\}=-\frac{QAL}{2}\begin{Bmatrix}1\\ 1\end{Bmatrix}, \tag{4}$$

where A is the area and L the length of the element. The system (3) is solved by finite differences in the

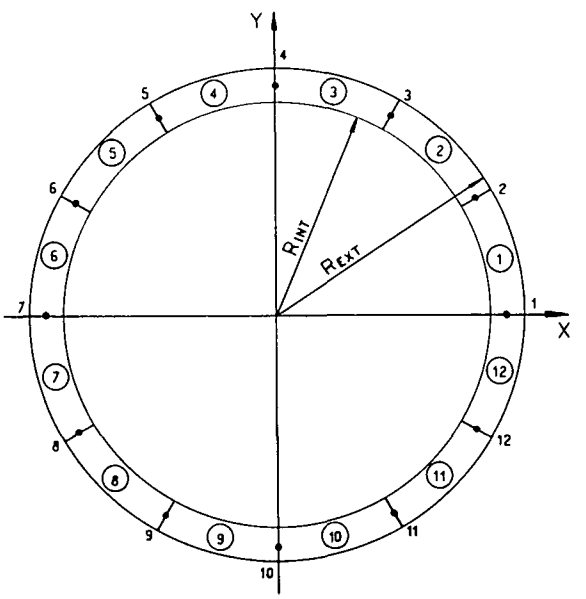

Fig. 1. The one dimensional finite element heat conduction model used for each of the tubes. The elements and the nodes are numbered. The numbers of the elements are encircled.

time domain using the Crank–Nicholson central difference scheme which is unconditionally stable [3]. The solution $\{T\}_{NEW}$ at the end of a time step Δt is obtained in terms of $\{T\}_{OLD}$ at the beginning of the time step by solving the following system of N linear algebraic equations:

$$(2[C] + [K]\,\Delta t)\{T\}_{NEW} = (2[C] - [K]\,\Delta t)\{T\}_{OLD} - 2\{F\}\,\Delta t\,. \quad (5)$$

In fact, eq. (5) as it stands was not useful for our purposes, because when the temperature distribution was close to equilibrium (e.g. at the end of a heating process), the heat flows Q were very small and so also was the vector $\{F\}$. In this situation $\{T\}_{NEW}$ results almost equal to $\{T\}_{OLD}$ and the temperature changes during a time step become comparable to the round-off errors introduced by the computer when solving the system (5). Curious effects were observed, as for example the temperature of the load did not converge to the constant external temperature but to a slightly different value. In order to overcome this difficulty we write:

$$\{T\}_{NEW} = \{T\}_{OLD} + \{\Delta T\}\,, \quad (6)$$

and we easily obtain from eq. (5):

$$(2[C] + [K]\,\Delta t)\{\Delta T\} = -2[K]\{T\}_{OLD}\,\Delta t - 2\{F\}\,\Delta t\,. \quad (7)$$

When this system of linear equations is solved, the round-off errors affect only the components of $\{\Delta T\}$, which are only small corrections to the actual temperature distribution $\{T\}_{OLD}$. Thus $\{T\}_{NEW}$ is calculated from eq. (6) with excellent accuracy.

3. Computer implementation of the finite element model

Since the thermal contacts between the tubes were all neglected, each finite element mesh is completely independent and can be solved separately. The computer program thus runs over all the tubes and solves eqs. (7) and (6) in each case by the following procedure. For each finite element, the heat conductivity K and the volumetric heat capacity ρc are calculated as function of the current average temperature of the element $T = (T_1 + T_2)/2$, where T_1 and T_2 are the two nodal temperatures of the element, by means of second-degree interpolating polynomials:

$$\rho c = a_1 + a_2 T + a_3 T^2\,, \quad (8)$$

$$K = a_4 + a_5 T + a_6 T^2\,. \quad (9)$$

The coefficients a_i, which depend on the material out of which the element is made and on the range of temperatures to be considered, are built into the program. The heat Q entering the element (see eq. (4)), is calculated by solving the radiation equations in the radiation enclosure to which the element belongs, as will be described later. The element matrices $[c^{(e)}]$, $[k^{(e)}]$ and vector $\{f^{(e)}\}$ are then calculated and assembled into $[A]$, $[K]$ and $\{F\}$. Sparse matrix technology [4] is a new method which allows for large savings in both computer storage requirements and processing time when dealing with matrix algebra. Sparse matrix technology is a standard feature in all our computer programs, and is therefore used to assemble the finite element matrices and vector [5]. The linear system (7) is then solved [6], using again sparse matrix procedures, and $\{T\}_{NEW}$ at the end of the time step is calculated from (6). The size of the time step is varied during the calculation. At the beginning, when large temperature gradients may be present in some regions of the mdoel, short steps are required. A convenient value was found to be 1 s. The time step is made progressively longer as the temperature gradients become smaller, up to a maximum of 20 s. Longer time steps were not tried.

4. Formulation of the radiation problem in enclosures

An enclosure is a closed region of space delimited by hot surfaces, where radiation phenomena take place. The surfaces are assumed to emit, and also to reflect the radiation which they receive, uniformly in all directions and independently of the wave-length (diffuse-gray surfaces). For the close-packed array of tubes, only two types of enclosures arise. The first is defined by three adjacent tubes in contact, and is approximated by 12 line segments, called *radiation sides*, as shown in fig. 2. Each radiation side is assigned a fixed temperature, equal to the temperature of the surface at the center of the side. For example, side 1 of fig. 3 is assigned the temperature

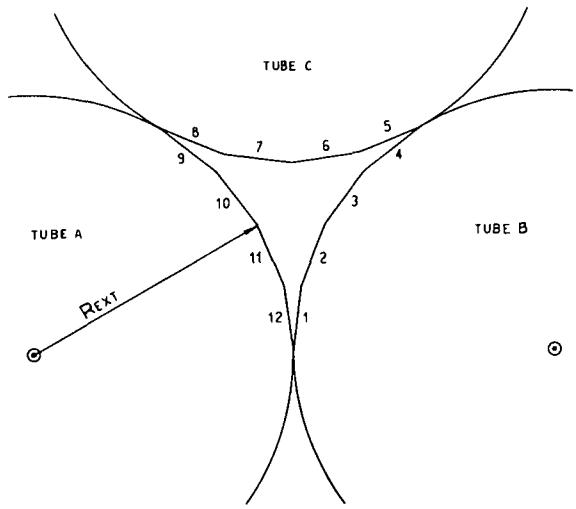

Fig. 2. The radiation enclosure defined by three adjacent tubes of outside radius R_{EXT} and approximated by 12 radiation sides. The radiation sides are numbered.

0.25 T_6(B) + 0.75 T_7(B), where T_6(B) and T_7(B) are the temperatures at the nodes 6 and 7 of tube B (see fig. 1) at the particular instant of time when the radiation problem is to be solved. Two radiation sides were assigned per finite element in order to represent more accurately the azimuthal temperature distribution around the tube circunference.

The second type of enclosure is the interior of a tube itself, a circular enclosure of radius R_{INT}. This enclosure was approximated by 24 radiation sides, two for each finite element. However, after several numerical experiments it was realized that the heat transfer by radiation in this enclosure was negligible when compared with the conduction of the tube wall. This is easily understood by comparing the fourth-power law of radiation with the linear law of conduction at the relatively low temperatures used for annealing. Consequently, the effect of the circular enclosure was disregarded in all subsequent calculations.

The radiation problem to be solved in an enclosure can now be stated as follows: given the temperatures of the radiation sides, determine the net heat flux which enters each side per unit of time as a result of the balance between the energy emitted and the energy absorbed by the side. Enclosure theory [7], Hottel's crossed-string method [8], and our general program are used to solve this problem. A matrix $[G]$ of viewfactors is first determined automatically for each type of enclosure. The element G_{ij} is the fraction of the heat emitted or reflected by the side i which reaches the side j. Its calculation requires a knowledge of whether the sides i and j face each other or not, and if they do, of the bodies which may be interposing partially or totally between both sides. In the general case of a multiply connected enclosure, such bodies may produce complicated shades and penumbra on the side j, or even determine several *channels* through which the radiation may flow from i to j. Given the geometry of the enclosure, for each pair i, j the computer program automatically determines the interposed bodies, generates all possible radiation channels, delimits each channel by two convex polygonals, finds the "cross-strings" (which are in fact limiting visuals) of Hottel [8] and calculates G_{ij}. Further details of the computer program will be given elsewhere.

Next, the following matrices are calculated for the enclosure;

$$[Z] = \{2[L] - ([I] - [A])[G]\}([I] - [A])\,, \quad (10)$$

$$[P] = \{2[A][L][Z]^{-1} - ([I] - [A])^{-1}\}\,\sigma[A][L]\,, \quad (11)$$

where

σ is Steffan's constant,

$[A]$ is a diagonal matrix whose elements are the emissivities of the sides,

$[L]$ is a diagonal matrix whose elements are the lengths of the sides, and

$[I]$ is the identity matrix.

The solution of the radiation problem stated above is given by the equation

$$\{q\} = [P]\{t\}\,, \quad (12)$$

where $\{t\}$ is a vector whose components are the fourth powers of the absolute temperatures of the sides, and $\{q\}$ is the vector of heat fluxes entering each side. The matrix $[P]$ depends on the emissivities of the surfaces which border the enclosure. The emissivities are assumed to be independent of the temperature for the present calculations. The matrix $[P]$ can thus be calculated for each type of enclosure once and for all, and then the relation (12) is used at each time step. The heat fluxes $\{q\}$ of the radiation

sides are assembled appropriately in order to obtain the finite element heat fluxes Q to be used in eq. (4).

5. Results and discussion

The techniques just discussed were applied to nine different cases with two different loads. The nine cases are described in table 1. The first load is composed of 210 tubes of zircaloy-4, with outside diameter of 1.19 cm and wall thickness of 0.055 cm, see fig. 3. We refer to such tubes as "small". The second load, shown in fig. 4, consists of 22 "large" tubes of 4.45 cm outside diameter and 0.762 cm wall thickness. The effect of the furnace was simulated by keeping the temperature at all the external nodes on the tubes at a constant value T_{EXT} during all the time steps. For example, the nodes 8, 9, 10, 11 and 12 (see fig. 1) of the tubes 2 through 11 (see fig. 3) were kept at the temperature T_{EXT}, and so also were the nodes 6–12 of the tube 1 and the nodes 6–10 of the tubes 13, 26, 40, etc. All the remaining nodes were assigned an initial temperature of T_{INIC}.

For a load composed of tubes with such thin walls as the small tubes, this way of simulating the effect of the furnace is quite realistic. If the load of fig. 3 is cold and is suddenly placed into a hot furnace at the temperature T_{EXT}, the external surfaces of all the external tubes will reach a temperature close to T_{EXT} in a time much shorter than the times required to transfer the heat to the internal tubes. For the large tubes this may not be the case, and it may be necessary to consider the time required to heat up the external tubes to a temperature near to T_{EXT}. A good estimation can be obtained by simply adding this time to the times reported in the plots, because of the following argument, which will be explained below: the heat proceeds to the interior of the load by heating up succesively each layer of tubes, and no one layer of tubes will heat up appreciably until the preceding layer has risen in temperature considerably.

A consequence of the model is that the external tubes will heat up very quickly by thermal conduction around their perimeters, and the evolution of their temperatures with time will not provide any information concerning the process of heat radiation. Therefore, we plot only the temperatures of tubes which belong to internal layers. Another consequence

Table 1
List of the cases discussed in this paper

Designation	Definition	Outside diameter (cm)	Wall thickness (cm)	Emissivity	Number of tubes	Initial temperature T_{INIC} (°C)	External temperature T_{EXT} (°C)	Model shown in fig.	Results given in fig.
HST	Heating of small tubes	1.19	0.055	0.229	210	20	500	3	5
HSDT	Heating of small dark tubes	1.19	0.055	0.700	210	20	500	3	5
PHST	Pre heating of small tubes	1.19	0.055	0.299	210	20	210	3	6
FHST	Final heating of small tubes	1.19	0.055	0.229	210	210	500	3	6
CST	Cooling of small tubes	1.19	0.055	0.229	210	500	20	3	5
HLT	Heating of large tubes	4.45	0.762	0.229	22	20	750	4	7
PHLT	Pre heating of large tubes	4.45	0.762	0.229	22	20	210	4	7
FHLT	Final heating of large tubes	4.45	0.762	0.229	22	210	750	4	7
CLT	Cooling of large tubes	4.45	0.762	0.229	22	750	20	4	7

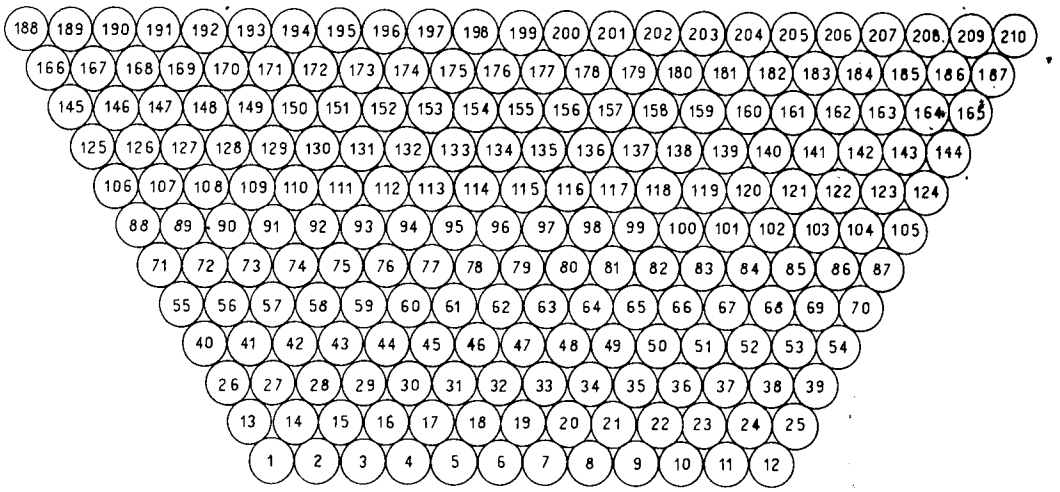

Fig. 3. Cross-section of the close-packed array of 210 "small" tubes. The tubes are numbered. The numerical results corresponding to this load are shown in figs. 5 and 6.

is that the total heat power input to the load, calculated from this model as a function of time, can not be expected to represent the function which would be measured by placing the cold load into an actual high vacuum furnace. Therefore, information on heat fluxes will be postponed until the results of the model of an actual furnace are communicated in a future publication.

The results presented here give a good idea of the general behaviour of a load placed in a high vacuum furnace, in particular of the time required for the heat to reach the internal elements of the load. Due to the simplicity of the present model, good physical insight can be obtained concerning the parameters which govern the propagation of the heat from element to element by radiation, and considerations of great value to the designer can be formulated.

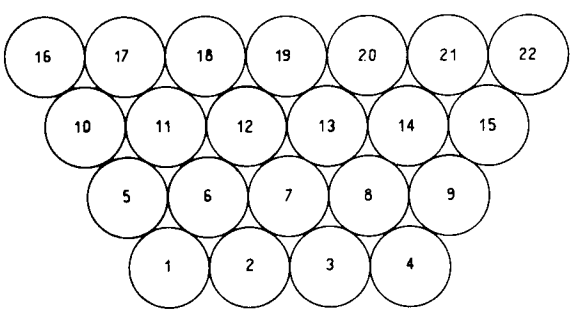

Fig. 4. Cross-section of the close-packed array of 22 "large" tubes. The tubes are numbered. The numerical results corresponding to this load are shown in fig. 7.

The first observed fact is that the amounts of heat transfered by radiation are small when compared with the conduction by the walls. A given tube may absorb heat from radiation at one side, conduct it to the other side and then radiate it again, but the temperature gradients developed by the conduction in the tube wall are small. The largest temperature difference that was observed between two opposed points on the same tube was 28°C, corresponding to the tubes 19 and 176 of the case HSDT (small dark tubes, emissivity = 0.700). Therefore, the concept of average temperature of a tube does have a physical meaning, and will be refered to as the "temperature" of the tube.

The results are shown in figs. 5, 6 and 7. Each curve is identified by the designation given in table 1 and a number which references the tube of fig. 3 or 4 whose temperature is plotted. Each selected tube is representative of an entire layer. For example, tube 19 of fig. 3 is representative of tubes 14–24, 27, 41, 56, etc. In fig. 5 are represented the numerical results for heating small tubes from 20 to 500°C, and for cooling from 500 to 20°C. Several important facts are observed here. Fore the case HST, when $t = 10$

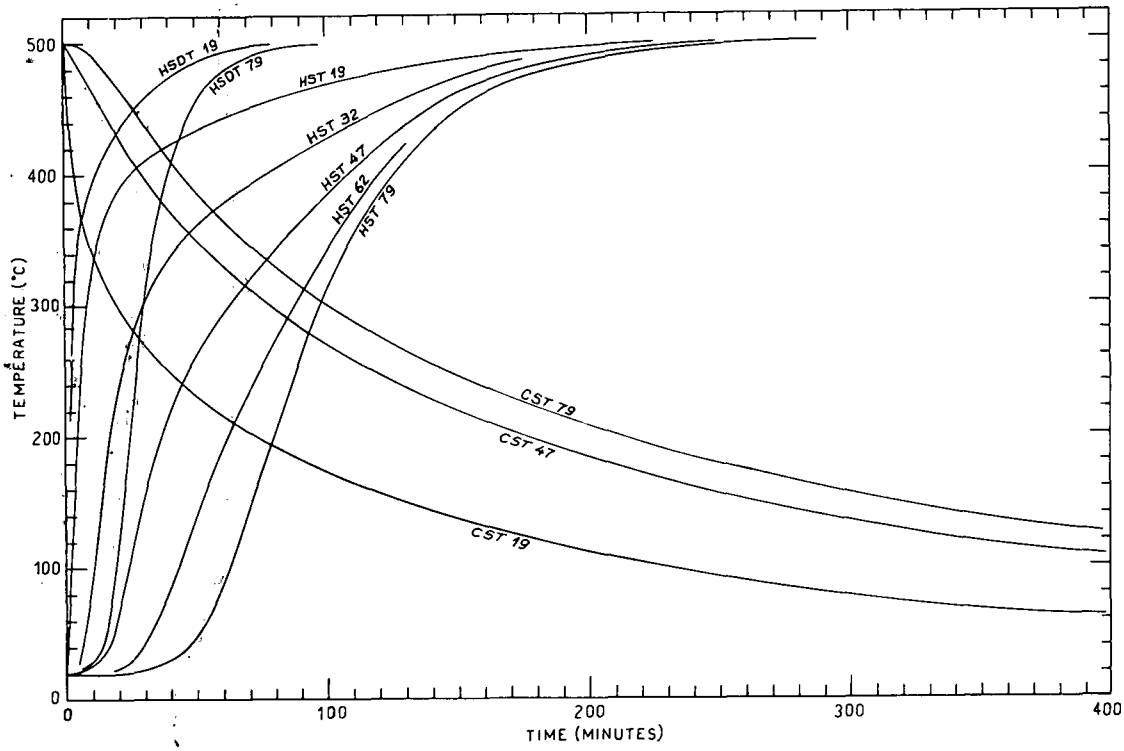

Fig. 5. Graph of the numerical results obtained for heating from 20 to 500°C and cooling from 500 to 20°C of the load of fig. 3. Heating curves are shown for two different emissivities of the surfaces of the tubes. The curves are identified in table 1. The numbers refer to the numbering of the tubes of fig. 3.

min the temperatures of the tubes 19, 32, 47, 62 and 79 are respectively: 325, 92, 26, 20 and 20°C. When t = 20 min the temperatures are 387, 234, 68, 23 and 20°C. These numbers illustrate the characteristic stepwise propagation of the heat to the interior of the load, layer by layer, which is a consequence of Stefan's fourth-power law: the heat flux radiated from a certain layer towards the next is appreciable only after the temperature of the layer has increased considerably. It is also a consequence of the relatively high reflectivity assumed for the surface: a large temperature difference is required between two adjacent layers in order that any appreciable amount of energy could be absorbed by the colder one.

Another fact observed in fig. 5 is the effect of increasing the emissivity (case HSDT). The times required by the innermost tube no. 79 to reach a temperature of 490°C when the emissivity is 0.700 or 0.229 are, respectively, 72 min and 220 min. This result is certainly the basis of a method for improving the yield of a furnace.

Fig. 5 also shows that the time required to cool down a load is much longer than that required to heat the same load over the same temperature interval. A comparison between the cases HST and CST shows that the tube 79 heats up from 130 to 450°C in only 85 min, while it takes 346 min to cool down the same tube from 450 to 130°C. This result is also a consequence of the fourth-power law of heat radiation and can be easily explained as follows. During the heating process, when tube 79 reaches a certain temperature T_0, other neighboring tubes, such as 62 and 63, are hotter, and are therefore much stronger radiators than a body at temperature T_0. A high energy flux is established from 62 and 63 to 79. On the other hand, during the cooling process, when tube 79 is at temperature T_0, tubes 62 and 63 are colder. The stronger radiator is now tube 79, which is at temperature T_0,

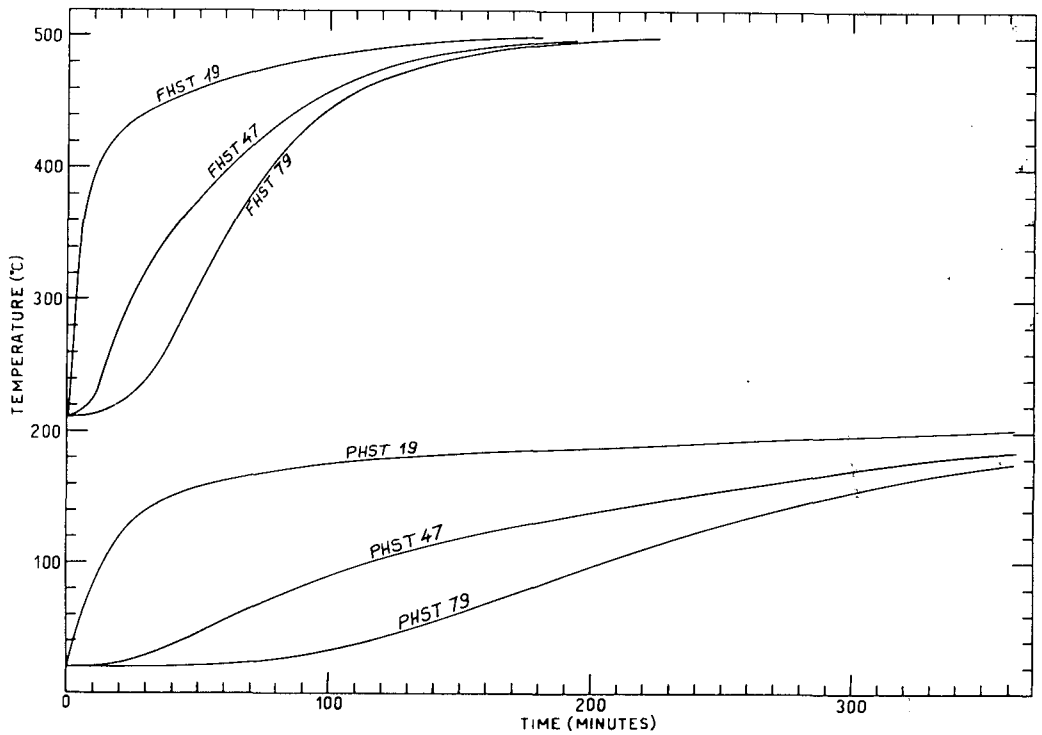

Fig. 6. Graph of the numerical results obtained for the pre-heating of the load of fig. 3 between the initial temperature of 20°C and an intermediate temperature of 210°C, and for the heating from 210°C, to the final temperature of 500°C. The curves are identified in table 1. The numbers refer to the numbering of the tubes of fig. 3.

and the heat flux from 79 to 62 and 63 will be low.

It is also possible to argue as follows. During heating, the external portion of the load is permanently at high temperatures, and as a result of the T^4 law, large amounts of heat radiation are available to heat up the colder portions of the load. On the other hand, a short time after the cooling of a hot load has started, no portion of the load will be at high temperatures, and the heat exchanges between hotter and colder portions will be much lower. This situation becomes worse as the load cools down.

The same arguments apply to the results shown in fig. 6. These results represent the anlysis of the idea of pre-heating the load in an auxiliary furnace in order to save time of operation of the main furnace. The pre-heating temperature was chosen to be 210°C, a value which was considered safe for zircaloy cladding in a low-priced furnace with poor or no temperature control. Fig. 6 shows that the pre-heating from 20 to 210°C takes a long time. Therefore, the auxiliary furnace must be a low-priced one in order that its use be economically convenient. Not much is gained, however, in time of operation of the main furnace. The curves labeled FHST show the final heating of the load, which is assumed to have an initial temperature of 210°C. The times required by the tube 79 to reach a temperature of 480°C are 190 and 141 min in figs. 5 and 6, respectively. For a temperature of 490°C the times are 220 and 169 min, and for 498°C, 285 and 225 min. A pre-heated load will be completely hot in about 50 to 60 min less time than a cold load. However, in practice, due to the exceedingly large time required for pre-heating, the center of the pre-heated load will be at a temperature somewhat lower than the pre-heating temperature, and the times required for the final heating will be longer than those reported. Our rough estimation is that not more than 30 min will be gained by

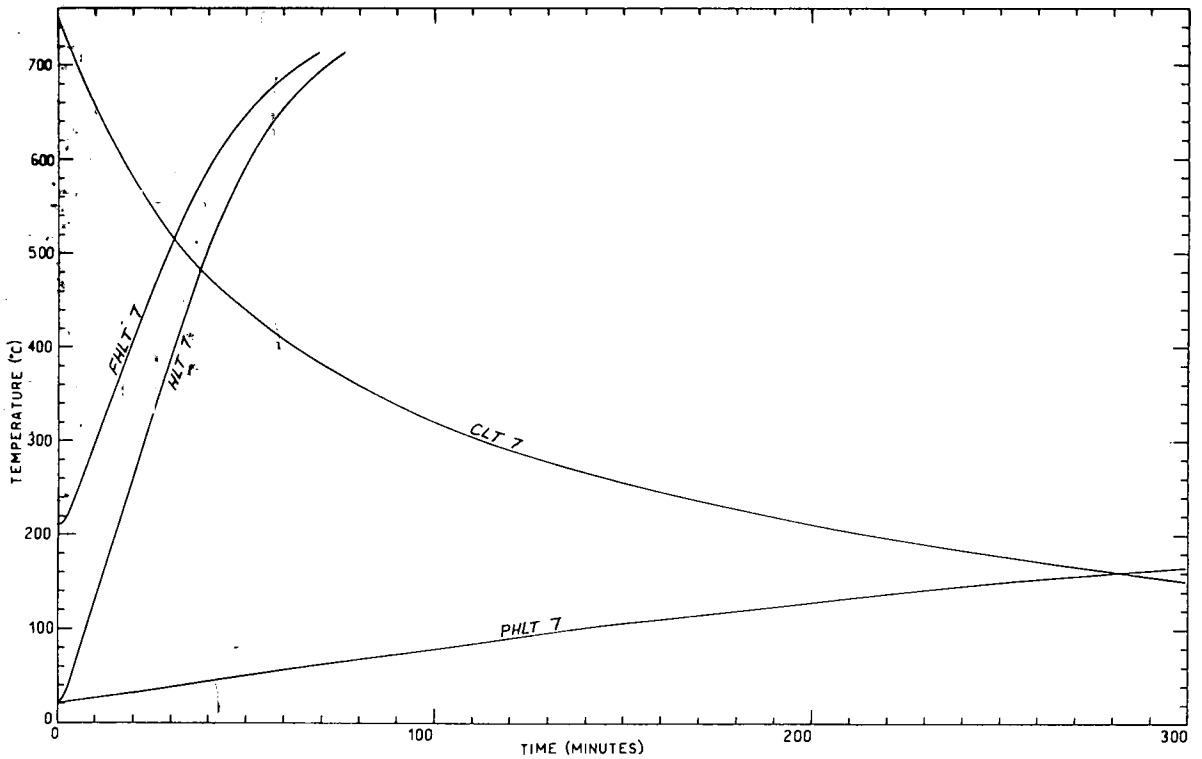

Fig. 7. Graph of the numerical results obtained for the load of fig. 4. The curves shown represent heating from 20 to 750°C, pre-heating from 20 to 210°C, heating from 210 to 750°C, and cooling from 750 to 20°C. The curves are identified in table 1 and correspond to the average temperature of the tube no. 7 of fig. 4.

pre-heating the load during 6 h at 210°C. Of course, an improvement in these figures can be achieved by setting the pre-heating temperature at a higher value, but in such a case the pre-heating furnace will require a more sophisticated and expensive design.

In fig. 7 are shown the results obtained for the load of large tubes of fig. 4. The general characteristics of these results are the same as those discussed above, except that the heating time is much shorter. This is due both to the smaller number of layers of tubes in the load, and to the higher temperature of the furnace (750°C). Another consequence of the same facts is that the time gained by pre-heating the load to 210°C is now much shorter: less than 10 min. Pre-heating the load does not seem to be convenient in any case.

Acknowledgement

The author wishes to thank H. Cingolani for many illuminating discussions concerning the computer program, J.C. Almagro for giving us the technical data and for his advice and numerous suggestions and N. Callwood for his careful reading of the manuscript.

References

[1] O.C. Zienkiewicz, The Finite Element method in Engineering Science (McGraw-Hill, London, 1971).
[2] L.J. Segerlind, Applied Finite Element Analysis (John Wiley, New York, 1976).
[3] J. Donea, Internat. J. Numer. Methods Engrg. 8 (1974) 103–110.
[4] D.J. Rose and R.A. Willoughby, Editors, Sparse Matrices and their Applications (Plenum Press, New York, 1972).

[5] F.G. Gustavson, R.C. 6176 (26569) IBM Thomas J. Watson Research Center (1976).
[6] S. Pissanetzky, CNEA-NT 15/78, Buenos Aires (1978).
[7] R. Siegel and J.R. Howell, Thermal Radiation Heat Transfer (McGraw-Hill, New York, 1972).
[8] H.C. Hottel, Radiant Heat Transmission, in: W.H. McAdams, Ed., Heat Transmission, McGraw-Hill, New York, 3rd ed. (1954) chap. 4.